Fluxons and their interactions in a system of three stacked Josephson junctions

C. Gorria,[1,2] P. L. Christiansen,[1] Yu. B. Gaididei,[1,3] V. Muto,[2] N. F. Pedersen,[4] and M. P. Soerensen[1]
[1]*Section of Mathematical Physics, IMM, Technical University of Denmark, DK-2800, Kongens Lyngby, Denmark*
[2]*Department of Applied Mathematics and Statistics, University of the Basque Country, E - 48080 Bilbao, Spain*
[3]*Bogolyubov Institute for Theoretical Physics, 252143 Kiev, Ukraine*
[4]*Department of Electric Power Engineering, Technical University of Denmark, DK-2800, Kongens Lyngby, Denmark*
(Received 21 November 2002; revised manuscript received 6 February 2003; published 17 July 2003)

Fluxon dynamics in a system of three coupled driven damped sine-Gordon equations is investigated. Bunching of fluxons is observed. It is shown that fluxon-fluxon-fluxon bound states exist in a certain interval of the fluxon velocity. Attraction between fluxons occurs as a result of indirect fluxon-fluxon interaction mediated by Swihart waves. To tackle the problem analytically a piece-wise linear approach is developed. The analytical approximations show good agreement with the results obtained by direct numerical simulations.

DOI: 10.1103/PhysRevB.68.035415 PACS number(s): 74.50.+r, 05.45.Yv, 85.25.Cp

I. INTRODUCTION

The fluxon dynamics in stacked long Josephson junctions have been investigated in detail during the last decade.[1–8] The possibility of comparing theoretical predictions with experimental measurements increases the interest of these systems. The potential applications of the vertical stacked Josephson junctions cover several interesting fields such as the design of devices for storage and transmission of electronic signals and high-frequency radiation emission and detection devices.

When two layers of superconducting material are separated by an insulating layer and overlap between Cooper pairs wave functions occurs, then Cooper pairs (as well as electrons) can cross the insulating barrier due to the tunneling effect. The dynamics of the phase difference φ between the wave functions in the two superconducting layers is governed by the perturbed sine-Gordon equation.

The sine-Gordon equation emerges from many different physical fields in the study of nonlinear wave phenomena.[9] Special care has to be taken in the study of stacked junctions as compared to a single junction due to the interaction effect between the stacked junctions. This interaction was first studied in the case of two junctions by Mineev *et al.*[10] and later it was widely investigated.[11–26] The symmetry between the two equations in the case of two junctions may hide some important aspects of the fluxon motion. In order to investigate the general properties of a system of an arbitrary number of junctions we study the case of three junctions. It is important to note the difference in the motion of fluxons in interior junctions, as 2 in Fig. 1, which receive interaction from their two neighboring junctions, 1 and 3, while the two exterior junctions only receive interaction from one neighboring junction. By simple arguments the topological dissimilarity between junctions is most important for $n=3$. In the limit $n=\infty$ all junctions are again similar topologically.

Our starting point is the model described by Sakai, Bodin, and Pedersen[2] where a theory describing the interaction between a general system of N junctions is deduced from the Maxwell, London, and Josephson equations. The equations for the particular case of three junctions are

$$J_1=\frac{1}{1-2S^2}[\varphi_{1,xx}-S\varphi_{2,xx}+S^2(\varphi_{3,xx}-\varphi_{1,xx})],$$

$$J_2=\frac{1}{1-2S^2}[\varphi_{2,xx}-S(\varphi_{1,xx}+\varphi_{3,xx})], \tag{1}$$

$$J_3=\frac{1}{1-2S^2}[\varphi_{3,xx}-S\varphi_{2,xx}+S^2(\varphi_{1,xx}-\varphi_{3,xx})],$$

where $J_i=\varphi_{i,tt}+\alpha\varphi_{i,t}+\sin\varphi_i+\gamma_i$, $i=1,2,3$. The electromagnetic interaction between adjacent junctions is expressed by a coupling constant S, and its physical value[2] belongs to the interval $-0.5<S\leqslant 0$. The constant α_i represents the damping and γ_i represents the driving force in the ith junction. Realistically due to physical requirements, the driving forces introduced into each junction must be the same, i.e., $\gamma_i=\gamma$, $i=1,2,3$, as shown in Fig. 1.

The Lagrangian of Eq. (1) for the undamped system, $\alpha=0$, is

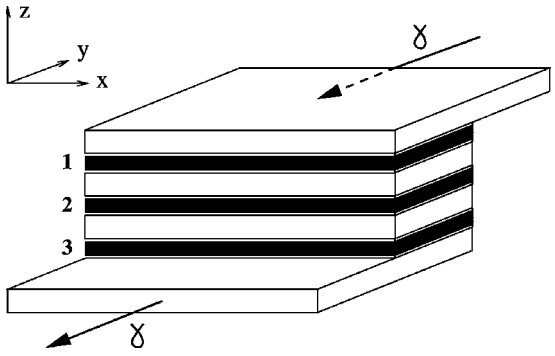

FIG. 1. Structure of the stack of four superconductors and three intermediate junctions (1,2,3). Unidirectional external bias is applied along the system.

$$L=\sum_{i=1}^{3}\int\left[\frac{1}{2}\varphi_{i,t}^{2}-\frac{1}{2(1-2S^{2})}\varphi_{1,x}^{2}-1+\cos\varphi_{i}\right]dx + \int\frac{S}{(1-2S^{2})}\varphi_{2,x}(\varphi_{1,x}+\varphi_{3,x})dx-\sum_{i=1}^{3}\int\gamma x\varphi_{i,x}dx. \tag{2}$$

The uncoupled and unperturbed system, $S=\alpha=\gamma=0$ in Eq. (1), reduces to three identical equations which allow a simple single soliton solution given by the expression

$$\varphi(x,t)=4\arctan\left[\exp\sigma\left(\frac{x-vt-x_{0}}{\sqrt{1-v^{2}}}\right)\right], \tag{3}$$

where v is the velocity of the wave. It is called a fluxon ($\sigma=1$) or an antifluxon ($\sigma=-1$), depending on the polarity. The maximum speed for one single equation ($n=1$) is the velocity of light in the junction, the so-called Swihart velocity,[27] c, which is used for normalization in the following. Several perturbation methods have been developed to study this model in detail.[28,29]

The aim of this paper is to investigate the trajectories and stability in (x,t) space and time of the single fluxons or antifluxons in each junction to determine stable modes. The stability analysis of the system of two junctions was studied by means of perturbation analysis of the antiphase linear mode by Grønbech-Jensen *et al.*[14,15] Assuming fluxon-type solutions in each junction, the coupling effect leads to repulsion between the center portion of the fluxons of identical polarity and attraction between the fluxons of opposite polarity. This conclusion is obtained investigating the minimum of the potential energy of the system. The basic ideas for this case were first established by Mineev *et al.*[10] and later several investigations, making use of the symmetry of this case, were performed.[11,13,17,19,21,30] On the other hand, a unidirectional γ force drives the fluxon and antifluxon in opposite directions.[28]

In the case of two stacked Josepson junctions, stable coherent in-phase zero-field steps in the current-voltage characteristic were observed experimentally in Refs. 17 and 31. An experimental finding of different cavity resonances (Fiske modes) in three stacked junctions was presented in Ref. 32. So far direct observation of coherent in-phase fluxon motion in three and more Josepson junctions has not been reported.[33]

Of physical interest are the modes where the waves excited in the top and bottom junctions are identical. Stable bunching of solitons are shown in Secs. II and III. Thus we will restrict our analysis to the fluxon-antifluxon-fluxon (f-a-f), $\sigma_1=1$, $\sigma_2=-1$ in Eq. (3), and fluxon-fluxon-fluxon (f-f-f), $\sigma_1=\sigma_2=1$, cases.

In Sec. II we develop piecewise linear approximations (PWLA's) of the fully nonlinear equations, substituting the $\sin\varphi_i$ term by linear approximations. In the f-a-f case the threshold between the driving and the coupling parameters for the bunched state is deduced. Otherwise the locked state of fluxons in the f-f-f case is possible only for a certain range of high speeds above the Swihart velocity[27] where oscillating tales are created in the fluxons.[11,13,15] These oscillations are successfully represented by the PWLA's and the threshold for bunching in the driving-damping parameter space is obtained for each value of the coupling constant with a good degree of accuracy. In one junction bunching only occurs in the presence of surface current loss.[34–39]

In Sec. III the method used for the numerical simulations is described. The solutions are shown for different parameters of the equation and compared to the analytical predictions. In Sec. IV the conclusions about the work are summarized.

In Appendix A, a collective coordinates approach is formulated. This method gives qualitatively good results when the fluxons are driven with low velocities and successfully predicts the bunching of different polarity fluxons but fails to predict the bunching of equal polarity ones. In Appendix B the particular symmetric configuration of two identical junctions is studied by the PWLA method. It is found that the fluxon-fluxon mode is stable above Swihart velocity and oscillating tales do not appear.

II. PIECEWISE LINEAR APPROXIMATION

The two modes (f-a-f) and (f-f-f) have physical relevance because they are the only ones which can be excited in stacked coupled Josephson junctions by a uniform bias current. Bunched states of fluxons may exist in both modes but the dynamics is completely different.

It is well known that bias current drives the fluxons and the antifluxon, Eq. (1) with $\sigma=1$ and $\sigma=-1$, respectively, in opposite directions.[28] For the case of a (f-a-f) mode it was shown quite recently[26] that in the framework of the collective coordinates approach the balance between the separation tendency due to driving force and the fluxon-antifluxon attraction may lead to a bunched state. In contrast to this the bunched state on the (f-f-f) mode does not exist.

As it has been shown[6,11,13,15,17,40] bunching of fluxons in the case of two Josephson junctions may be explained beyond the collective coordinates approach. High amplitude radiation, which is attractive for the fluxons of neighboring junctions, is created when these fluxons move in the range of velocity, v, between the Swihart velocities, $c_{-}<v<c_{+}$, where $c_{\pm}=1/(1\pm\sqrt{2}S)^{1/2}$ are the asymptotic phase velocities of the small amplitude linear plasma waves.[8,41,42]

General solutions for the fully nonlinear coupled system, Eqs. (1), are not known. We are interested in traveling-wave-type solutions, $\varphi_i(x,t)=\varphi_i(z)$, where $z=x-vt$. Taking into account that in both modes, (f-a-f) and (f-f-f), fluxons in the first and the third junctions are identical, the set of Eqs. (1) can be reduced to the following two equations:[23,24]

$$(\mu^{2}-v^{2})\varphi_{1}''(z)+\alpha v\varphi_{1}'(z)-\sin\varphi_{1}(z)-2S\mu^{2}\varphi_{2}''(z)-\gamma=0,$$
$$(\mu^{2}-v^{2})\varphi_{2}''(z)+\alpha v\varphi_{2}'(z)-\sin\varphi_{2}(z)-S\mu^{2}\varphi_{1}''(z)-\gamma=0, \tag{4}$$

where $\mu^{2}=1/(1-2S^{2})=c_{-}^{2}\cdot c_{+}^{2}$.

We cannot solve Eqs. (4) analytically. Therefore to provide some insight into the physical mechanism of fluxon interaction, we use PWLA's, $P(\varphi_i)$, for the nonlinear terms, $\sin\varphi_i$, in order to linearize Eqs. (4) in a piecewise fashion.

Here we present two choices, P_a and P_m, for the operator P,

$$P_a(\varphi)=\begin{cases} a\varphi, & \text{for} \quad 0\leqslant\varphi<\pi, \\ a(\varphi-2\pi), & \text{for} \quad \pi\leqslant\varphi<2\pi, \end{cases} \tag{5}$$

and

$$P_m(\varphi)=\begin{cases} \varphi, & \text{for} \quad 0\leqslant\varphi<\pi/2, \\ \pi-\varphi, & \text{for} \quad \pi/2\leqslant\varphi<3\pi/2, \\ \varphi-2\pi, & \text{for} \quad 3\pi/2\leqslant\varphi<2\pi, \end{cases} \tag{6}$$

respectively.

The first one, $P_a[\varphi(z)]$, is the simpler. As seen in Fig. 2(a) it provides a good representation of the fluxon tails as $\varphi\rightarrow 0$ or 2π. However, it is discontinuous at $\varphi=\pi$. The free parameter a $(0<a\leqslant 1)$ controls the slopes of the approximating straight lines and may be used to adapt the approximation.

The second one, $P_m[\varphi(z)]$, is more accurate. It was used[43] to describe fluxon dynamics in a single junction with a surface loss term. As seen in Fig. 5(a) below $P_m(\varphi)$ provides a good approximation to the fluxon tails as $\varphi\rightarrow 0$ or 2π and also to the center portion of the fluxons at $\varphi\approx\pi$. In contrast to P_a, P_m is continuous.

The analytical solutions obtained by substituting $\sin\varphi$ by $P_m(\varphi)$ are more accurate than using P_a but also more cumbersome. In the following sections the reasons for choosing between the two approximations are given.

A. Fluxon-antifluxon-fluxon

Here we describe the (f-a-f) bunching taking into account fluxon shape modification. Because we are interested in the low velocity case, where v is much smaller than the lowest Swihart velocity, c_-, we may use the PWLA, P_a, given by Eq. (5).

The identical bias term, γ, in all junctions, Eq. (1), drives the fluxons in one direction and the antifluxon in the opposite one. On the other hand due to coupling between junctions the fluxons and the antifluxon attract each other.[11,13,21,22] As a result of the competition between driving and interaction of junction coupling the fluxons and the antifluxon are separated by the distance, d. For $\gamma>0$ the antifluxon is behind the fluxons and the distance between them, d, increases with the driving force. Thus in the framework of the PWLA one should distinguish the following three intervals as shown in Fig. 2(b):

$$\begin{aligned} &\text{(I)} \quad z\leqslant 0\Leftrightarrow 2\pi\geqslant\varphi_2>\pi, \\ &\text{(II)} \quad 0<z\leqslant d\Leftrightarrow\varphi_2\leqslant\pi, \quad \varphi_1<\pi, \\ &\text{(III)} \quad d<z\Leftrightarrow\pi\leqslant\varphi_1\leqslant 2\pi. \end{aligned} \tag{7}$$

Inserting solutions of the type $\varphi_i(z)=D_i e^{\lambda z}-\gamma/a$ in the linear system of the ODE, Eq. (4) with $P=P_a$, the corresponding fourth-order characteristic equation is obtained to be

$$\left[\left(\frac{1}{1-2S^2}-v^2\right)\lambda^2+\alpha v\lambda-a\right]^2=\frac{2S^2}{(1-2S^2)^2}\lambda^4. \tag{8}$$

The roots of Eq. (8) are

$$\lambda_{1,2}=-p_+\pm\sqrt{p_+^2+aq_+}, \quad \lambda_{3,4}=-p_-\pm\sqrt{p_-^2+aq_-}, \tag{9}$$

where the terms $p_\pm$ and $q_\pm$ are

$$p_\pm=\frac{\alpha v}{2(c_\pm^2-v^2)}, \quad q_\pm=\frac{1}{(c_\pm^2-v^2)}. \tag{10}$$

The eigenvectors (D_1,D_2) associated to the solution of the linear system will be $(1,\sqrt{2})^T$ and $(1,-\sqrt{2})^T$, corresponding to the in-phase and antiphase modes. For low velocities, $|v|<c_1$, $\lambda_{1,3}$ are positive and $\lambda_{2,4}$ are negative. The expressions for the bounded solutions of the piecewise linearized version of Eq. (4) in each one of the three regions, I, II and III, become

$$\text{(I)}\begin{cases} \hat{\varphi}_1(z)=H_1e^{\lambda_1 z}+H_2e^{\lambda_3 z}-\dfrac{\gamma}{a}, \\ \hat{\varphi}_2(z)=\sqrt{2}(H_1e^{\lambda_1 z}-H_2e^{\lambda_3 z})+2\pi-\dfrac{\gamma}{a}, \end{cases} \tag{11}$$

$$\text{(II)}\begin{cases} \hat{\varphi}_1(z)=G_1e^{\lambda_1 z}+G_2e^{\lambda_2 z}+G_3e^{\lambda_3 z}+G_4e^{\lambda_4 z}-\dfrac{\gamma}{a}, \\ \hat{\varphi}_2(z)=\sqrt{2}(G_1e^{\lambda_1 z}+G_2e^{\lambda_2 z}-G_3e^{\lambda_3 z}-G_4e^{\lambda_4 z})-\dfrac{\gamma}{a}, \end{cases} \tag{12}$$

$$\text{(III)}\begin{cases} \hat{\varphi}_1(z)=K_1e^{\lambda_2 z}+K_2e^{\lambda_4 z}+2\pi-\dfrac{\gamma}{a}, \\ \hat{\varphi}_2(z)=\sqrt{2}(K_1e^{\lambda_2 z}-K_2e^{\lambda_4 z})-\dfrac{\gamma}{a}. \end{cases} \tag{13}$$

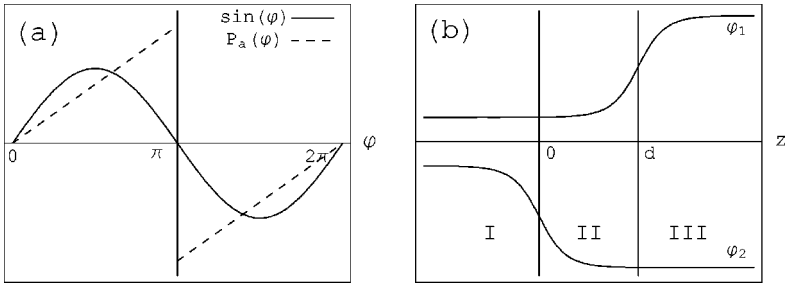

FIG. 2. (a) Piecewise linear approximation $P_a[\varphi(z)]$ (dashed curve) of the $\sin\varphi(z)$ function (full curve) with $a=0.7$. (b) $\varphi_1=\varphi_3$ are displaced ahead a distance d from φ_2, forced by the bias current, γ.

The eight constants $(H_1,H_2,G_1,G_2,G_3,G_4,K_1,K_2)$ are determined by the ten matching conditions at the points $z=0$ and $z=d$,

$$\hat{\varphi}_2^I(0)=\hat{\varphi}_2^{II}(0)=\hat{\varphi}_1^{II}(d)=\hat{\varphi}_1^{III}(d)=\pi,$$

$$\hat{\varphi}_1^I(0)=\hat{\varphi}_1^{II}(0), \quad \hat{\varphi}_2^{II}(d)=\hat{\varphi}_2^{III}(d), \tag{14}$$

$$\frac{d\hat{\varphi}_i^I(0)}{dz}=\frac{d\hat{\varphi}_i^{II}(0)}{dz}, \quad \frac{d\hat{\varphi}_i^{II}(d)}{dz}=\frac{d\hat{\varphi}_i^{III}(d)}{dz}, \quad i=1,2,$$

where the superscripts $(\cdots)^I$, $(\cdots)^{II}$, and $(\cdots)^{III}$ indicate the regions I, II, or III, respectively, in which the function is evaluated and the apostrophe indicates differentiation with respect to z.

By using any eight from the ten matching conditions, Eqs. (14), the eight constants $(H_1,H_2,G_1,G_2,G_3,G_4,K_1,K_2)$ may be expressed as functions of the parameters S, γ, α, and v. The remaining two conditions give the dependence of the distance between solitons, d, and the relation between the velocity, v, and the driving force, γ. After some algebraic calculations we get simple expressions for these two remaining conditions as a function of the coefficients G_1 and G_3 given by Eqs. (14) to be

$$\left(\frac{\lambda_1}{\lambda_2}-1\right)e^{\lambda_1 d}G_1=-\pi, \quad \left(\frac{\lambda_3}{\lambda_4}-1\right)e^{\lambda_3 d}G_3=-\pi. \tag{15}$$

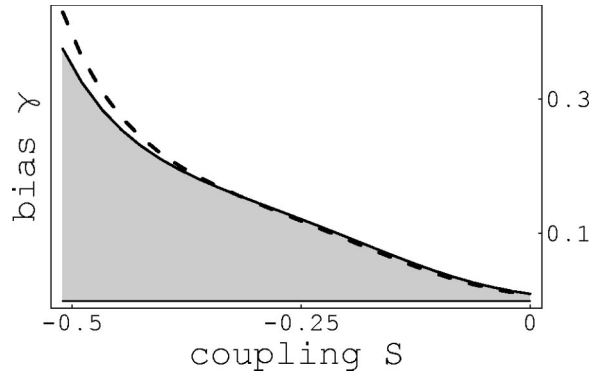

FIG. 3. The gray shaded area indicates the region in the (S,γ)-parameter space in which bunching of the (f-a-f) occurs in the numerical simulations. The dashed curve draws the contour of the region in which the PWLA of the (f-a-f) leads to bunching for the free parameter $a=0.5$.

When the coupling parameter, S, is large enough to counteract breakup induced by the driving force, γ, Eqs. (15) have finite solutions for the velocity, v, and distance, d. This means that the bunched state of the (f-a-f) mode exists. The corresponding phase diagram in the (S,γ) space is presented in Fig. 3.

The PWLA, Eq. (11), reproduces quite accurately the shape of the fluxons for the weak bias current, γ, where the bunching of the (f-a-f) occurs, as is shown in Fig. 4. On the other hand at high bias current, γ, when the fluxons move with velocity close to the lowest Swihart velocity, c_-, the shape of the fluxons are more sensitive to variations[44] and this simple discontinuous PWLA, Eq. (5), is not sufficiently accurate. It reproduces accurately the behavior of fluxons in the tails but is not correct at the center portion of the fluxons which significantly contribute to the fluxon interaction. In this case we need the more accurate approximation given by Eq. (5) to obtain the bunched (f-f-f) state in the following section.

B. Fluxon-fluxon-fluxon

In the framework of the collective coordinates approach the bunched state of three fluxons is unstable (see Appendix A). Fluxons repel each other and the potential energy of interaction, U_{int}, decreases when the distance between fluxons increases. However, as it follows from the results of numerical simulations[11,13,15,23,24,45] (see also below) the bunched state does exist when the driving force exceeds some critical value. It is also quite remarkable that an appearance of bunched states is *always* accompanied by cre-

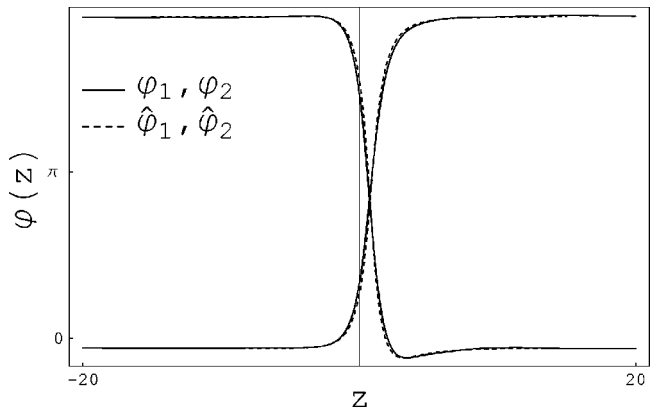

FIG. 4. Bunched fluxons and antifluxon from the numerical simulation (full curve) and PWLA (dashed curve). $S=-0.49$, $\alpha=0.1$, $\gamma=0.2$, and $a=0.5$ have been used.

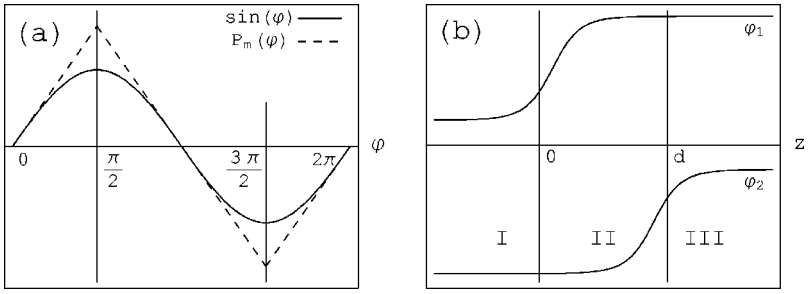

FIG. 5. (a) Piecewise linear approximation $P_m[\varphi(z)]$ (dashed curve) of the $\sin\varphi(z)$ function (full curve). (b) Fluxon, φ_2, forwarded a distance d from the fluxon, φ_1, due to the interaction from its two neighbors.

ation of oscillatory tails of fluxons. The bunched state of equal polarity fluxons in coupled Josephson junctions is always related to these oscillatory tales unless there are only two junctions with the same physical properties. The symmetry of this configuration, which may be considered as degenerate, provides a fluxon-fluxon solution without oscillations as is deduced in Appendix B. Therefore to describe fluxon bunching one should use an approach which takes into account the change of shape of fluxons and appearance of oscillating tails. This can be done in the framework of the PWLA. The approximation P_a given by Eq. (5) is too crude in the central portion of the fluxon to provide the bunched state. Instead the more accurate P_m, given by Eq. (6) and shown in Fig. 5(a), is used. We assume that the fluxon in the interior junction, φ_2, travels slightly ahead by a distance d with respect to the fluxons of junctions 1 and 3, $\varphi_1=\varphi_3$, as shown in Fig. 5(b).

As in the previous section we distinguish three intervals for the PWLA,

$$\text{(I)}\ z\leqslant 0\Leftrightarrow 0<\varphi_1\leqslant\frac{\pi}{2},$$

$$\text{(II)}\ \ 0<z\leqslant d\Leftrightarrow\varphi_1>\frac{\pi}{2},\quad \varphi_2\leqslant\frac{3\pi}{2}, \tag{16}$$

$$\text{(III)}\ \ d<z\Leftrightarrow\frac{3\pi}{2}<\varphi_2\leqslant 2\pi.$$

Inserting solutions of the type $\varphi_i(z)=D_i e^{\lambda z}\pm\gamma$ ($-$ in regions I and III and $+$ in region II) into the linear system of the ODE obtained from Eq. (4) substituting $\sin\varphi_i\rightarrow P_m(\varphi_i)$ we get the characteristic equations

$$\left[\left(\frac{1}{1-2S^2}-v^2\right)\lambda^2+\alpha v\lambda\mp 1\right]^2=\frac{2S^2}{(1-2S^2)^2}\lambda^4. \tag{17}$$

The upper sign ($^-$) corresponds to regions I and III and the lower sign ($+$) to region II. The roots of Eq. (17) in regions I and III are

$$\overline{\lambda}_{1,2}=-p_+\pm\sqrt{p_+^2+q_+},\quad \overline{\lambda}_{3,4}=-p_-\pm\sqrt{p_-^2+q_-}, \tag{18}$$

where $p_\pm$ and $q_\pm$ are given by Eq. (10). For speeds higher than the Swihart velocity, $v>c_-$, the roots $\overline{\lambda}_{3,4}$ become complex and they are responsible for the emergence of oscillatory tails of the fluxons. For convenience we denote $\overline{\lambda}_{3,4}=\overline{\lambda}_r\pm i\overline{\lambda}_l$, where $\overline{\lambda}_r=-p_-$ and $\overline{\lambda}_l=\sqrt{-(p_-^2+q_-)}$ are real. In region II the roots are

$$\overline{\lambda}_{5,6}=-p_+\pm\sqrt{p_+^2-q_+},\quad \overline{\lambda}_{7,8}=-p_-\pm\sqrt{p_-^2-q_-}. \tag{19}$$

The roots $\overline{\lambda}_{7,8}$ are real while $\overline{\lambda}_{5,6}$ are complex; for convenience we denote $\overline{\lambda}_{5,6}=\overline{\lambda}_m\pm i\overline{\lambda}_h$, where $\overline{\lambda}_m=-p_+$ and $\overline{\lambda}_h=\sqrt{-(p_+^2-q_+)}$ are real. In the three regions the eigenvalues corresponding to the solution of the characteristic equations are $(D_1,D_2)=(1,\sqrt{2})$ and $(D_1,D_2)=(1,-\sqrt{2})$ for the in-phase and the antiphase modes, respectively. The bounded solutions of the linearized version of Eq. (4) in regions I, II, and III become

$$\text{(I)}\begin{cases}\hat{\varphi}_1(z)=\overline{H}_1e^{\overline{\lambda}_1 z}+e^{\overline{\lambda}_r z}(\overline{H}_2\cos\overline{\lambda}_l z+\overline{H}_3\sin\overline{\lambda}_l z)-\gamma,\\ \hat{\varphi}_2(z)=\sqrt{2}[\overline{H}_1e^{\overline{\lambda}_1 z}-e^{\overline{\lambda}_r z}(\overline{H}_2\cos\overline{\lambda}_l z-\overline{H}_3\sin\overline{\lambda}_l z)]-\gamma,\end{cases} \tag{20}$$

$$\text{(II)}\begin{cases}\hat{\varphi}_1(z)=e^{\overline{\lambda}_m z}(\overline{G}_1\cos\overline{\lambda}_h z+\overline{G}_2\sin\overline{\lambda}_h z)+\overline{G}_3e^{\overline{\lambda}_7 z}+\overline{G}_4e^{\overline{\lambda}_8 z}+\pi+\gamma,\\ \hat{\varphi}_2(z)=\sqrt{2}[e^{\overline{\lambda}_m z}(\overline{G}_1\cos\overline{\lambda}_h z+\overline{G}_2\sin\overline{\lambda}_h z)-\overline{G}_3e^{\overline{\lambda}_7 z}-\overline{G}_4e^{\overline{\lambda}_8 z}]+\pi+\gamma,\end{cases} \tag{21}$$

$$\text{(III)}\begin{cases}\hat{\varphi}_1(z)=\overline{K}_1e^{\overline{\lambda}_2 z}+2\pi-\gamma,\\ \hat{\varphi}_2(z)=\sqrt{2}(\overline{K}_1e^{\overline{\lambda}_2 z})+2\pi-\gamma.\end{cases} \tag{22}$$

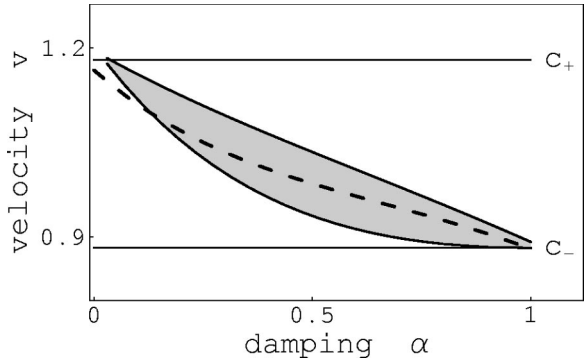

FIG. 6. The gray shaded area indicates the region in the parameter space (α,γ) for $S=-0.2$, where bunching of the (f-f-f) occurs in the numerical simulations. The bottom contour of this region is approximated by the PWLA (dashed line) but the top contour cannot be found by this approach.

The eight constants $(\overline{H}_1,\overline{H}_2,\overline{H}_3,\overline{G}_1,\overline{G}_2,\overline{G}_3,\overline{G}_4,\overline{K}_1)$ are determined by the ten matching conditions at the points $z=0$ and $z=d$, and the corresponding equations are

$$\hat{\varphi}_1^I(0)=\hat{\varphi}_1^{II}(0)=\frac{\pi}{2},\quad \hat{\varphi}_2^{II}(d)=\hat{\varphi}_2^{III}(d)=\frac{3\pi}{2},$$

$$\hat{\varphi}_2^I(0)=\hat{\varphi}_2^{II}(0),\quad \hat{\varphi}_1^{II}(d)=\hat{\varphi}_1^{III}(d), \tag{23}$$

$$\frac{d\hat{\varphi}_i^I(0)}{dz}=\frac{d\hat{\varphi}_i^{II}(0)}{dz},\quad \frac{d\hat{\varphi}_i^{II}(d)}{dz}=\frac{d\hat{\varphi}_i^{III}(d)}{dz},\quad i=1,2.$$

The remaining two conditions can be written in the following way as functions of $\overline{G}_1$ and $\overline{G}_4$ obtained previously by Eqs. (23):

$$\left(\frac{e^{\overline{\lambda}_m d}}{\cos\overline{\lambda}_h d}\right)\overline{G}_1=\left(\frac{\overline{\lambda}_m+\dfrac{\overline{\lambda}_2}{\sqrt{2}}}{\overline{\lambda}_h}-\tan\overline{\lambda}_h d\right)\left(\gamma-\frac{\pi}{2}\right),$$

$$\left(\frac{\overline{\lambda}_8}{\overline{\lambda}_7}-1\right)e^{\overline{\lambda}_8 d}\overline{G}_4=\left(1-\frac{1}{\sqrt{2}}\right)\left(\gamma-\frac{\pi}{2}\right). \tag{24}$$

From Eqs. (24) the values of the distance between fluxons, d, and the velocity, v, are fixed as function of the parameters S, α, and γ. Solving Eqs. (24) for each coupling constant, S, we obtain the region in the (α,γ)-parameter space where bunching in the (f-f-f) mode exists. Figure 6 shows this region calculated numerically between the Swihart velocities, $c_-<v<c_+$, where bunching exists. The bottom contour of this region may be approximated by the PWLA, while the top contour of the region cannot be approximated by the PWLA, due to creation of new pairs of fluxon-antifluxons above this contour. The PWLA, Eqs. (20)–(22), reproduces quite accurately the shape of the fluxons for low values of the driving force, γ, where the bunching of the (f-a-f) takes place, as shown in Fig. 7.

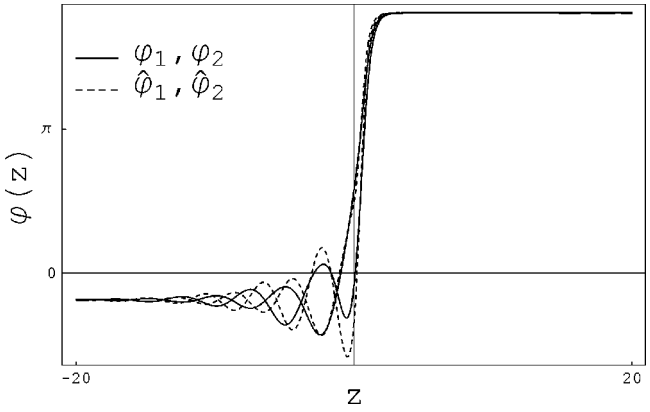

FIG. 7. Bunched fluxons from the numerical simulation (full curve) and as result of the PWLA (dashed curve). The parameters are $S=-0.2$, $\alpha=0.2$, and $\gamma=0.6$. The velocity is $v=1.1>c_-$. One can see good agreement between both results.

III. NUMERICAL SIMULATIONS

A symmetric central finite difference method of second order for both space and time has been implemented for the numerical simulations. The total length of the junctions is $L=40$ and the spatial mesh size is $\Delta x=0.05$. We have chosen periodic boundary conditions, $\varphi_i(L/2)=\varphi_i(-L/2)+2\pi$ and $\varphi_{i,x}(L/2)=\varphi_{i,x}(-L/2)$, $i=1,2,3$, corresponding to an annular geometry to avoid ambiguities due to reflection from edges.

As shown in previous sections, in the antiphase mode (f-a-f) the fluxons and the antifluxons are attracted by the coupling between junctions while a bias current of the same sign in all fluxons, γ, drives them in opposite directions. When the coupling is strong enough to overcome the fluxon-antifluxon separation caused by the bias term the two fluxons and the antifluxon will travel bunched, as is shown in Fig. 8(a), while a higher driving force will lead to a split in the fluxons, as is shown in Fig. 8(b). The bunching in the (f-a-f) mode takes place for $|v|<c_-$.

The numerical simulations have been made under fixed values of the coupling constant, S, and the dissipation, α, and varying the driving, γ. A numerically found dependence of the bias current vs fluxon velocities is plotted in Fig. 6.

The (f-f-f) mode presents a more complex scenario than the (f-a-f). Here the bunching is possible for speeds between the lowest and the highest Swihart velocities, $c_-<v<c_+$. Thus the simulations have been made for a high driving force, γ. Three types of fluxon motion have been detected. When γ is lower than a threshold value the bunched state does not exist. Fluxons in external junctions split from the fluxon in the internal junction [see Fig. 9(a)] and they propagate with different velocities.

Increasing the bias parameter, γ, we find the range of values where bunched states exists. This bunching interval depends on the coupling S and the dissipation α. When bunching takes place the fluxons move their centers with the same velocity, v, belonging to the interval (c_-,c_+), and their centers are separated by a small distance, as is shown in Fig. 9(b). The emergence of oscillating tails in the numerical solution of Eq. (1) for this high velocity, v, induces the three

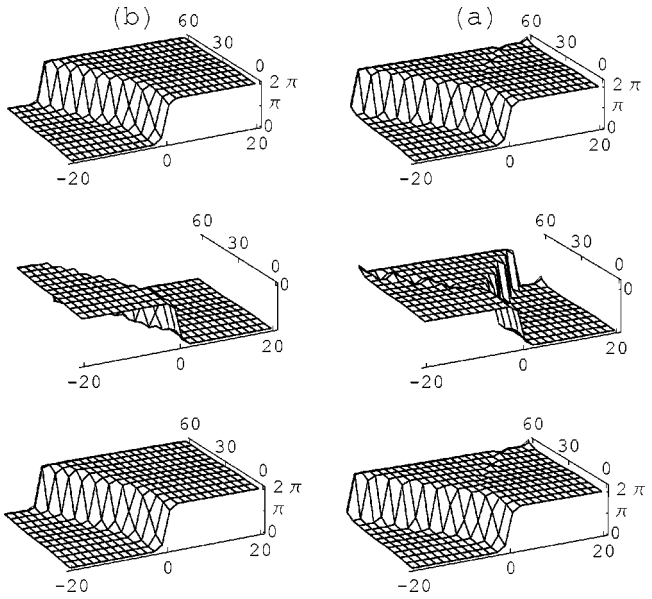

FIG. 8. Three-dimensional graphics of the behavior in time of the (f-a-f) mode. (a) The (f-a-f) mode splits for coupling, $S=-0.2$ and bias current, $\gamma=0.1$. (b) The (f-a-f) bunched mode for coupling $S=-0.2$ and bias current $\gamma=0.09$.

fluxons to bunch. For a too high bias [$\gamma=0.69$ in Fig. 9(c)] the equilibrium of bunching is broken by the creation of a new pair of fluxon-antifluxon.[46]

It is worth mentioning that fluxon splitting is an irreversible process. For example, having initially a bunched state, one can destroy it by decreasing the bias term, γ, and crossing the bottom contour in Fig. 5. As a result exterior fluxons and the interior one split off and start to move with different velocities. It is impossible to rebunch these fluxons by increasing the driving force, γ.

The bias current versus the numerically found fluxon velocities (i.e., the *I-V* curve with voltage replaced by velocity) are plotted in Fig. 10. When the fluxons move more slowly than c_-, they split and travel with different velocities, $\varphi_1=\varphi_3$ with v_1 and φ_2 with v_2, where $v_1<v_2$. Bunching state branches are observed in narrow ranges of velocities between c_- and c_+.

As was mentioned above we used a uniform driving force, γ. Therefore during the simulations we did not observe a mode corresponding to a fluxon in the first junction, nothing in the second, and an antifluxon in the third, which was proved to be stable in the no-bias, no-damping case.

IV. CONCLUSIONS

We have investigated a theoretical model of three coupled Josephson junctions taking into account identical fluxons, $\varphi_1=\varphi_3$, in exterior junctions and a fluxon or antifluxon in the interior one, φ_2. In the case of (f-a-f) the interaction between the fluxons leads to repulsion between the center portion of the fluxons and antifluxon while the bias term, γ, drives them in opposite directions. The combination of these two factors gives rise to bunching or unbunching depending on the balance between S and γ. The simple analytical

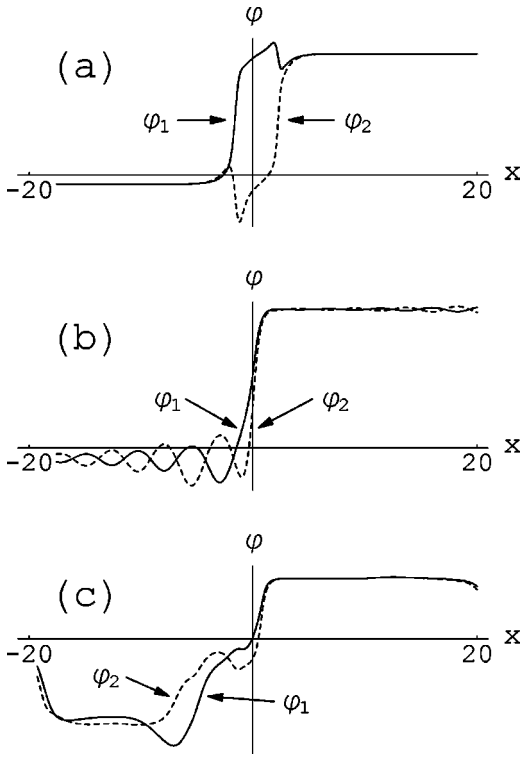

FIG. 9. Behavior of fluxons φ_1 (full curve) and φ_2 (dashed curve) for coupling $S=-0.2$, damping $\alpha=0.1$, and bias current. (a) $\gamma=0.43$ fluxons split with velocities $v_1=0.868$ for φ_1 and $v_2=0.88$ for φ_2; (b) $\gamma=0.44$ bunched fluxons with velocity $v_1=v_2=1.118$; (c) $\gamma=0.69$ creation of a new fluxon-antifluxon pair due to excess energy.

PWLA used, $\sin\varphi\rightarrow P_a(\varphi)$, gave successful results in the approximation of the shapes of the solutions as well as in the determination of the region in (S,γ) phase space where bunching occurs. This method gives better results than the collective coordinates approach because it works well even when the range of velocities is not restricted to slow ones, $|v|\gg 0$.

The behavior of the waves in the (f-f-f) mode is notori-

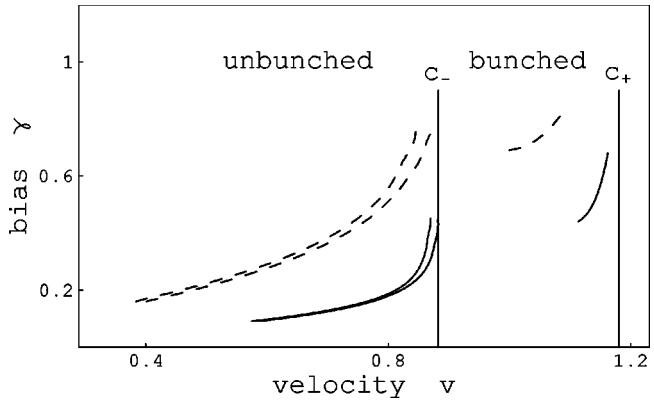

FIG. 10. Bias current, γ, versus fluxon velocity, v, for coupling for $S=-0.2$. Full (dashed) curves represent velocity versus bias for $\alpha=0.1$ ($\alpha=0.3$). Below c_-, fluxons split and two different velocity branches are observed for φ_1 and φ_2. Fluxon bunching occurs in a velocity interval between c_- and c_+.

ously different than the previous one. Here the interaction coupling induces repulsion between the fluxons for speeds below the lowest Swihart velocity, $v<c_-$. In the high velocity regime, $c_-<v<c_-$, the fluxon bunching may exist only for a certain range of velocities due to the creation of an oscillating tales mirror symmetric in the fluxons of adjacent junctions. These oscillations provide the internal energy of a local minimum when the fluxons are separated by a small distance, *d*. Under these conditions the changes of the shapes of the fluxons are very sensitive to small variations of the parameters and that is why we have chosen the more sophisticated PWLA, $\sin\varphi\rightarrow P_m(\varphi)$. The analytical solutions obtained by this method approximate accurately the solutions given by the numerical simulations and also give approximately the lower velocity threshold for the bunched state. This result cannot be obtained by the classical method of collective coordinates (see Appendix A) because the oscillating tales, which are fundamental for the bunching, are not taken into account in the classical fluxon type of trial functions. *I-V* curves have been calculated numerically in order to clarify the behavior of the fluxons inside the bunching interval of the parameter space (S,γ), as well as outside this interval.

ACKNOWLEDGMENT

C.G. and Yu.B.G. acknowledge the hospitality of the Technical University of Denmark, where the investigations were performed and N.F.P. acknowledges support from the ESF (VORTEX program) and the Danish STVF program (New Superconductors). Financial support was provided by the Marie Curie Fellowship Program (Grant No. HPMT-CT-2001-00402) and a project from the University of the Basque Country (Grant No. UPV/EHU 100.310-E-13891/2001).

APPENDIX A: COLLECTIVE COORDINATES

In this Appendix the attraction between the center portions of the fluxon and the antifluxon in the (f-a-f) mode and the repulsion between the fluxons in the (f-f-f) mode is investigated. The standard procedure is to study the minima of the potential energy, *W*, as a function of the distance between the waves in the different junctions.

In the collective coordinate approach generalized coordinates defined by $\vec{q}(t)=[q_1(t),\ldots,q_n(t)]$ are used. They determine the position of the particles at time *t*. The energy of the system given by Eq. (1) may be written in terms of these coordinates, *q*, and their derivatives with respect to time, $\dot{q}$. The potential energy, *W*, will depend only on *q*, while the kinetic energy, *T*, will depend on *q* and $\dot{q}$. Using the standard procedure[47,48] we obtain from the Lagrangian (2) the equations of motion for each of the generalized coordinates, $q_i(t)$,

$$\frac{\partial L}{\partial q_j}-\frac{d}{dt}\frac{\partial L}{\partial \dot{q}_j}=2\alpha\sum_{i=1}^{3}\int \varphi_{i,t}\frac{\partial\varphi_i}{\partial q_j}dx. \tag{A1}$$

The natural choice of the generalized coordinates for Eq. (1) is $\vec{q}(t)=\vec{X}(t)=[X_1(t),X_2(t),X_3(t)]$, where X_i is the center of the *i*th fluxon, φ_i, and $u_i\equiv\dot{X}_i$ is the velocity of the center. The fluxon solutions of the unperturbed single sine-Gordon equation are used as trial functions,

$$\varphi_i(x,t)=4\arctan\left\{\exp\sigma_i\left[\frac{x-X_i(t)}{l_i}\right]\right\}, \tag{A2}$$

where $l=\sqrt{1-u_i^2(t)}$ is the width of the waves, in accordance with the Lorentz contraction. In order to simplify the equations of motion, we assume identical widths, $l_i=l$, as is indeed the case for traveling waves with low velocities, $|u_i|\ll 1$.

All the contributions except the terms which involve φ_j vanish from the partial derivatives of the Lagrangian with respect to X_j and $\dot{X}_j$,

$$\frac{\partial L}{\partial X_i}-\frac{d}{dt}\frac{\partial L}{\partial \dot{X}_i}=\int\left(2\alpha\varphi_{i,t}\frac{\partial\varphi_i}{\partial X_i}-\gamma x\frac{\partial\varphi_{i,x}}{\partial X_i}\right)dx. \tag{A3}$$

Substituting the expression of the fluxons, Eq. (A2), into Eq. (A1) and solving the integrals involved in Eq. (A3) we obtain the equations of motion for X_1 and X_2. The repulsion or the bunching effect will be determined by checking the relative distance between the center portion of the solitons.[11,13,22] This magnitude is defined as $Y=(X_1-X_2)/l$. Using symmetry arguments to calculate the involved integrals, the equation of motion for the distance, *Y*, is calculated in the same manner as[26]

$$\ddot{Y}+2\alpha\dot{Y}=\frac{3\sigma_1\sigma_2 S}{1-2S^2}\frac{d}{dY}\left(\frac{Y}{\sinh Y}\right)+\frac{\pi l\gamma}{4}(\sigma_1-\sigma_2). \tag{A4}$$

1. Fluxon-antifluxon-fluxon ($\sigma_1=-\sigma_2=1$)

Choosing the mode (f-a-f) the potential of Eq. (A4) leads to

$$V(Y)=\frac{3S}{1-2S^2}\frac{Y}{\sinh Y}-\frac{\pi l\gamma Y}{2}. \tag{A5}$$

The zeros of the derivative of the potential, $dV(Y)/dY$, determine the stationary points of the system, and they are located at the roots of the nonlinear equation,

$$\frac{3S}{1-2S^2}\left(\frac{1}{\sinh Y}-\frac{Y\cosh Y}{\sinh^2 Y}\right)-\frac{\pi l\gamma}{2}=0. \tag{A6}$$

A high value of the coupling parameter, *S*, compared with the driving force, γ, provide two extremes, $y_1<y_2$, for the potential. The first one, y_1, is a minimum (stable state) and the second one, y_2, is a maximum (unstable state). This means that the collective coordinates approach predicts attraction between the solitons of different polarities. They travel slightly separated by a distance y_1, which depends on the coupling parameter, *S*, and the driving force, γ.

2. Fluxon-fluxon-fluxon ($\sigma_1=\sigma_2=1$)

The potential corresponding to the wave configuration (f-f-f) can be reduced to

$$V(Y)=\frac{3S}{1-2S^2}\frac{Y}{\sinh Y}. \tag{A7}$$

There is only one finite zero of $dV(Y)/dY$ at $y_0=0$, which is a maximum of the potential. There are two zeros, $y_{1,2}=\pm\infty$, which are minima. The consequence is that the system reaches stationary states only when the fluxons are infinitely separated. Thus, the collective coordinates approach predicts the repulsion between the solitons of the same polarity.

APPENDIX B: PIECEWISE APPROXIMATION OF THE (F-F) MODE IN TWO JUNCTIONS

The particular case of two junctions with one fluxon traveling in each of them has been studied in detail in several publications.[11,13,15,23,24] Whenever the coupling parameter S is the same in both junctions, the equations of motion for both junctions are identical,

$$(\tilde{\mu}^2-v^2)\varphi_i''(z)+\alpha v\,\varphi_i'(z)-\sin\varphi_i(z)-S\tilde{\mu}^2\varphi_j''(z)-\gamma=0, \tag{B1}$$

where $i=1,j=2$ or $i=2,j=1$ and $\tilde{\mu}^2=1/(1-S^2)$. Due to symmetry of the system, Eq. (B1), both the in-phase mode $\varphi_1=\varphi_2$ and the antiphase mode $\varphi_1=-\varphi_2$ are solutions with maximum limit velocities $\tilde{c}_-=1/\sqrt{1-S}$ and $\tilde{c}_+=1/\sqrt{1+S}$, respectively.

In the numerical simulations the stability of the bunched state of the in-phase mode for a certain range of velocities is observed in the same manner as in the case of three junctions, which has been analyzed above. The particularity arises from the fact that in the case of two junctions with identical coupling, oscillating tales no longer appear. We apply the PWLA to Eq. (B1) in the same manner as in previous section. The roots of the corresponding characteristic equations for solutions of the type $\varphi_i(z)=D_ie^{\lambda z}$ and velocities higher than c_- are

$$\begin{aligned}
\tilde{\lambda}_{1,2}&=-\tilde{p}_+\pm\sqrt{\tilde{p}_+^2+\tilde{q}_+},\\
\tilde{\lambda}_{3,4}&=-\tilde{p}_-\pm\sqrt{\tilde{p}_-^2+\tilde{q}_-}=\tilde{\lambda}_r\pm i\tilde{\lambda}_l,\\
\tilde{\lambda}_{5,6}&=-\tilde{p}_+\pm\sqrt{\tilde{p}_+^2-\tilde{q}_+}=\tilde{\lambda}_m\pm i\tilde{\lambda}_h,\\
\tilde{\lambda}_{7,8}&=-\tilde{p}_-\pm\sqrt{\tilde{p}_-^2-\tilde{q}_-},
\end{aligned} \tag{B2}$$

where

$$\tilde{p}_\pm=\frac{\alpha v}{2(\tilde{c}_\pm-v^2)},\quad \tilde{q}_\pm=\frac{1}{(\tilde{c}_\pm-v^2)}. \tag{B3}$$

The eigenvectors, (D_1,D_2), are $(1,1)$ and $(1,-1)$ for the in-phase and antiphase modes, respectively.

Three regions, I, II and III, are distinguished in z space and the expressions of the fluxons in each region read

$$\text{(I)}\begin{cases}\hat{\varphi}_1(z)=\tilde{H}_1e^{\tilde{\lambda}_1z}+e^{\tilde{\lambda}_rz}(\tilde{H}_2\cos\tilde{\lambda}_lz+\tilde{H}_3\sin\tilde{\lambda}_lz)-\gamma,\\ \hat{\varphi}_2(z)=\tilde{H}_1e^{\tilde{\lambda}_1z}-e^{\tilde{\lambda}_rz}(\tilde{H}_2\cos\tilde{\lambda}_lz-\tilde{H}_3\sin\tilde{\lambda}_lz)-\gamma,\end{cases} \tag{B4}$$

$$\text{(II)}\begin{cases}\hat{\varphi}_1(z)=e^{\tilde{\lambda}_mz}(\tilde{G}_1\cos\tilde{\lambda}_hz+\tilde{G}_2\sin\tilde{\lambda}_hz)+\tilde{G}_3e^{\tilde{\lambda}_7z}+\tilde{G}_4e^{\tilde{\lambda}_8z}+\pi+\gamma,\\ \hat{\varphi}_2(z)=e^{\tilde{\lambda}_mz}(\tilde{G}_1\cos\tilde{\lambda}_hz+\tilde{G}_2\sin\tilde{\lambda}_hz)-\tilde{G}_3e^{\tilde{\lambda}_7z}-\tilde{G}_4e^{\tilde{\lambda}_8z}+\pi+\gamma,\end{cases} \tag{B5}$$

$$\text{(III)}\begin{cases}\hat{\varphi}_1(z)=\tilde{K}_1e^{\tilde{\lambda}_2z}+2\pi-\gamma,\\ \hat{\varphi}_2(z)=\tilde{K}_1e^{\tilde{\lambda}_2z}+2\pi-\gamma.\end{cases} \tag{B6}$$

The matching conditions which provide continuity and differentiability to the piecewise solutions are the same as Eqs. (23). Solving eight of this conditions we realize that some coefficients vanish,

$$\tilde{H}_2=\tilde{H}_3=\tilde{G}_3=\tilde{G}_4=0. \tag{B7}$$

Two conclusions are obtained from Eq. (B7). The first is that the two fluxons are identical, $\hat{\varphi}_1=\hat{\varphi}_2$, and the second is that there are no oscillating tales, $\dot{H}_2=\dot{H}_3=0$.

It is important to note that the cancellation of the four coefficients, Eq. (B7), arises from the fact that Eq. (B1) does not change with the choice of i and j subindexes. Otherwise if any one of the physical quantities, coupling, damping, or dissipation, change in one of the junctions the solutions given by piecewise approximations produce different fluxons, and oscillating tales exist in the case of three junctions.

[1] R. Kleiner, F. Steinmeyer, G. Kunkel, and P. Müller, Phys. Rev. Lett. **68**, 2394 (1992).
[2] S. Sakai, P. Bodin, and N.F. Pedersen, J. Appl. Phys. **73**, 2411 (1993).
[3] M. Tachiki, T. Koyama, and S. Takahashi, *Coherence in High Temperature Superconductors* (World Scientific, Singapore, 1996), p. 371.
[4] A.V. Ustinov and S. Sakai, Appl. Phys. Lett. **73**, 686 (1998).
[5] R. Kleiner, T. Gaber, and G. Hechtfischer, Physica C **362**, 29 (2001).
[6] V.M. Krasnov and D. Winkler, Phys. Rev. B **56**, 9106 (1997).
[7] M. Machida, T. Koyama, and M. Tachiki, Physica C **362**, 16 (2001).
[8] S. Sakai, A.V. Ustinov, H. Kohlstedt, A. Petraglia, and N.F. Pedersen, Phys. Rev. B **50**, 12 905 (1994).
[9] Y.S. Kivshar and B.A. Malomed, Rev. Mod. Phys. **61**, 763 (1989).
[10] M.B. Mineev, G.S. Mkrtchyan, and V.V. Schmidt, J. Low Temp. Phys. **45**, 497 (1981).
[11] Y.S. Kivshar and B.A. Malomed, Phys. Rev. B **37**, 9325 (1988).
[12] N. Grønbech-Jensen, M.R. Samuelsen, P.S. Lomdahl, and J.A. Blackburn, Phys. Rev. B **42**, 3976 (1990).
[13] N. Grønbech-Jensen, D. Cai, and M.R. Samuelsen, Phys. Rev. B **48**, 16 160 (1993).
[14] N. Grønbech-Jensen, P.S. Lomdahl, and M.R. Samuelsen, Phys. Rev. B **48**, 6353 (1993).
[15] N. Grønbech-Jensen, D. Cai, A.R. Bishop, A.W.C. Lau, and P.S. Lomdahl, Phys. Rev. B **50**, 6352 (1994).
[16] N. Grønbech-Jensen, J.A. Blackburn, and M.R. Samuelsen, Phys. Rev. B **53**, 12 364 (1996).
[17] A.V. Ustinov and H. Kohlstedt, Phys. Rev. B **54**, 6111 (1996).
[18] G. Carapella, G. Costabile, A. Petraglia, N.F. Pedersen, and J. Mygind, Appl. Phys. Lett. **69**, 1300 (1996).
[19] A. Wallraff, E. Goldobin, and A.V. Ustinov, J. Appl. Phys. **80**, 6523 (1996).
[20] G. Carapella, G. Costabile, S. Sakai, and N.F. Pedersen, Phys. Rev. B **58**, 6497 (1998).
[21] G. Carapella, Phys. Rev. B **59**, 1407 (1999).
[22] G. Carapella, G. Costabile, R. Latempa, G. Filatrella, and J. Mygind, Phys. Rev. B **62**, 9095 (2000).
[23] E. Goldobin, A. Wallraff, and A.V. Ustinov, J. Low Temp. Phys. **119**, 589 (2000).
[24] E. Goldobin, B.A. Malomed, and A.V. Ustinov, Phys. Rev. B **62**, 1414 (2000).
[25] F.K. Abdullaev, A.A. Abdumalikov, Jr., O. Buisson, and E.N. Tsoy, Phys. Rev. B **62**, 6766 (2000).
[26] P. Woafo, Phys. Lett. A **302**, 137 (2002).
[27] J.C. Swihart, J. Appl. Phys. **32**, 461 (1961).
[28] D.W. McLaughlin and A.C. Scott, Phys. Rev. A **18**, 1652 (1978).
[29] Y. Tang and W. Wang, Phys. Rev. E **62**, 8842 (2000).
[30] E. Goldobin, A. Wallraff, N. Thyssen, and A.V. Ustinov, Phys. Rev. B **57**, 130 (1998).
[31] E. Goldobin, M.Y. Kupriyanov, I.P. Nevirkovets, A.V. Ustinov, M.G. Blamire, and J.E. Evetts, Phys. Rev. B **58**, 15 078 (1998).
[32] A.V. Ustinov, H. Kohlstedt, M. Cirillo, N.F. Pedersen, G. Hallmanns, and C. Heiden, Phys. Rev. B **48**, 10 614 (1993).
[33] A.V. Ustinov, Physica D **123**, 315 (1998).
[34] P.L. Christiansen, P.S. Lomdahl, A.C. Scott, O.H. Soerensen, and J.C. Eilbeck, Appl. Phys. Lett. **39**, 108 (1981).
[35] P.S. Lomdahl, O.H. Soerensen, P.L. Christiansen, A.C. Scott, and J.C. Eilbeck, Phys. Rev. B **24**, 7460 (1981).
[36] S. Pagano, M.P. Soerensen, P.L. Christiansen, and R.D. Parmentier, Phys. Rev. B **38**, 4677 (1988).
[37] B.A. Malomed, Phys. Rev. B **47**, 1111 (1993).
[38] M.P. Soerensen, B.A. Malomed, A.V. Ustinov, and N.F. Pedersen, Physica D **68**, 38 (1993).
[39] I.V. Vernik, N. Lazarides, M.P. Soerensen, A.V. Ustinov, N.F. Pedersen, and V.A. Oboznov, J. Appl. Phys. **79**, 7854 (1996).
[40] E. Goldobin, H. Kohlstedt, and A.V. Ustinov, Appl. Phys. Lett. **68**, 250 (1996).
[41] A. Petraglia, Ph.D. thesis, Technical University of Denmark, 1996.
[42] N.F. Pedersen, Supercond. Sci. Technol. **15**, 405 (2002).
[43] S. Sakai and N. F. Pedersen, Phys. Rev. B **34**, 3506 (1986).
[44] V.M. Krasnov and D. Winkler, Phys. Rev. B **60**, 13 179 (1999).
[45] C. Gorria, P.L. Christiansen, Y.B. Gaididei, V. Muto, N.F. Pedersen, and M.P. Soerensen, Phys. Rev. B **66**, 172503 (2002).
[46] M. Peyrard and D. Kruskal, Physica D **14**, 88 (1984).
[47] L. D. Landau and E. M. Lifshitz, *Course of Theoretical Physics. Mechanics* (Pergamon, Bristol, 1960), Vol. I, pp. 3 and 76.
[48] J.G. Caputo, N. Flytzanis, and M.P. Soerensen, J. Opt. Soc. Am. B **12**, 139 (1995).